

See discussions, stats, and author profiles for this publication at: <https://www.researchgate.net/publication/46280401>

# Electrogenerated Chemiluminescent Anion Sensing: Selective Recognition and Sensing of Pyrophosphate

ARTICLE *in* ANALYTICAL CHEMISTRY · OCTOBER 2010

Impact Factor: 5.64 · DOI: 10.1021/ac1017293 · Source: PubMed

---

CITATIONS

29

---

READS

50

## 4 AUTHORS, INCLUDING:



**Ik-Soo Shin**

Soongsil University

27 PUBLICATIONS 641 CITATIONS

SEE PROFILE



**Se Won Bae**

Korea Institute of Industrial Technology, C...

10 PUBLICATIONS 207 CITATIONS

SEE PROFILE



**Hasuck Kim**

Seoul National University

134 PUBLICATIONS 4,227 CITATIONS

SEE PROFILE

# Electrogenerated Chemiluminescent Anion Sensing: Selective Recognition and Sensing of Pyrophosphate

Ik-Soo Shin, Se Won Bae, Hasuck Kim, and Jong-In Hong\*

Department of Chemistry, College of Natural Sciences, Seoul National University, Seoul 151-747, Korea

Recently, significant advances have been made independently in electrogenerated chemiluminescence (ECL) analysis and supramolecular anion sensing. Herein, we demonstrate a new proof of concept for ECL-based pyrophosphate (PPi) sensing, where the emission intensity is changed by electrochemical turn-on. The ECL PPi sensor (**1-2Zn**) consists of two orthogonally bonded moieties: boron dipyrromethene (ECL reporter) and a phenoxo-bridged bis( $\text{Zn}^{2+}$ –dipicolylamine) complex (PPi receptor). The presence of PPi is confirmed from the change in the intensity of green ECL generated from the former when PPi is selectively recognized by the latter. During PPi recognition, changes are caused in the electronic states of the receptor, and this stimulates the attenuation of ECL intensity. The electrochemical “on–off” triggering of light emission upon anion binding forms the basis of a new anion sensing strategy. We expect that green-colored ECL sensing would offer an advantage to current ECL analysis.

Anions play an important role in a wide range of biological, chemical, and environmental processes. Inorganic pyrophosphates (PPi) have been researched extensively because of their ubiquity in biology and widespread use in various industrial applications. Tin pyrophosphate ( $\text{Sn}_2\text{P}_2\text{O}_7$ ), for example, has recently received significant attention as a new negative electrode material for lithium batteries,<sup>1</sup> and vanadyl pyrophosphate ( $(\text{VO})_2\text{P}_2\text{O}_7$ ) has been recognized as an efficient catalyst for the oxidation of *n*-butane to maleic anhydride.<sup>2</sup> PPi, an environment pollutant, is the most common cause of cultural eutrophication.<sup>3</sup> From the biological viewpoint, PPi is involved in energy transduction and in the control of metabolic processes in organisms via participation in various enzymatic reactions.<sup>4</sup> For example, PPi is released in the formation of phosphodiester bonds during DNA polymerization and 3',5'-cyclic adenosine monophosphate (cyclic AMP, second messenger) synthesis and in the formation of activated intermediates (aminoacyl-tRNA) during protein

synthesis.<sup>5</sup> Patients with calcium pyrophosphate dihydrate (CPPD) crystal deposition disease and chondrocalcinosis have high levels of PPi in the synovial fluid.<sup>6</sup> PPi generated during the telomerase elongation step also indicates the activity of telomerase, which is a promising biomarker in the diagnosis and therapy of cancer.<sup>7</sup> Hence, the detection of PPi has been the main focus of several studies in the past decade, and particular attention has been paid to the development of fluorescent sensors for PPi. Thus far, only two methods of PPi detection have been reported. One is a bioluminescence method, which involves the analysis of fluorometric signals corresponding to the amount of Pi or ATP released in enzymatic cascade reactions involving PPi.<sup>8</sup> The other is a small-molecule chemosensor-based method in which fluorometric (and/or colorimetric) signals corresponding to the amount of PPi are analyzed; in this method, host–guest supramolecular complexes with PPi anions are employed.<sup>9</sup> Our group has developed chemosensors for PPi or phosphate-containing biomolecules.<sup>10</sup>

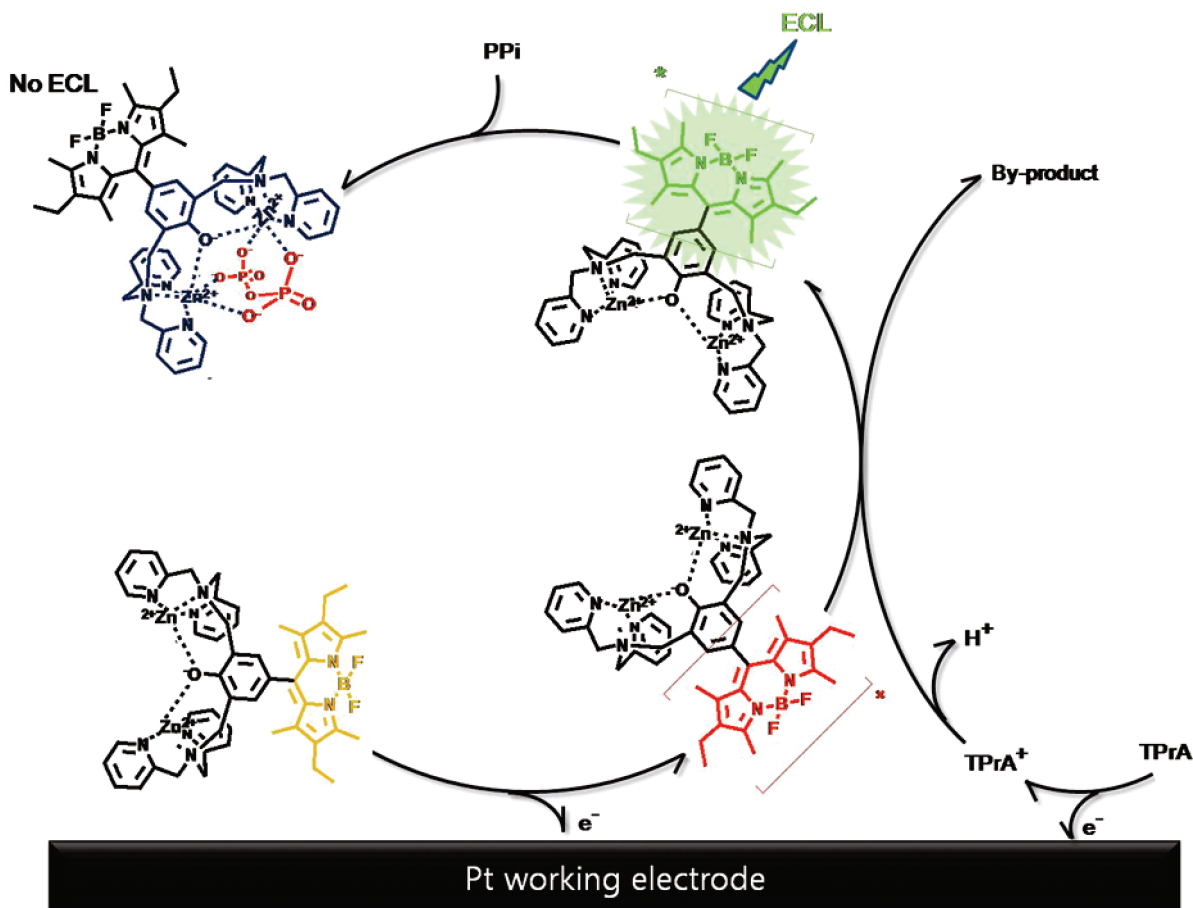
In this paper, we present a new proof of concept for PPi sensing, in which a synthetic organic molecule (**1-2Zn**) selectively recognizes PPi (Scheme 1); the PPi concentration is determined on the basis of changes in light emission under electrochemical turn-on. **1-2Zn** produces green electrogenerated chemiluminescence (ECL) in acetonitrile solution (MeCN), whose intensity varies with the PPi concentration. In ECL, the molecules on the electrode surface are excited (the excited states are formed at the electrodes) by an electron-transfer reaction between redox

\* To whom correspondence should be addressed. E-mail: jihong@snu.ac.kr.

- (1) Xiao, Y. W.; Lee, J. Y.; Yu, A. S.; Liu, Z. L. *J. Electrochem. Soc.* **1999**, *146*, 3623–3629.
- (2) *Kirk–Othmer Encyclopedia of Chemical Technology*, 4th ed.; Felthouse, T. R., Burnett, J. C., Mitchell, S. F., Mummy, M. J., Eds.; John Wiley & Sons: New York, 1998.
- (3) Lund, J. W. G. *Nature* **1974**, *249*, 797–797.
- (4) (a) Wilcox, D. E. *Chem. Rev.* **1996**, *96*, 2435–2458. (b) Cleland, W. W.; Hengge, A. C. *Chem. Rev.* **2006**, *106*, 3252–3278.

- (5) (a) Tabary, T.; Ju, L.-Y.; Cohen, J. H. M. *J. Immunol. Methods* **1992**, *156*, 55–60. (b) King, J. D.; Fitch, A. C.; Lee, J. K.; McCane, J. E.; Mak, D. D.; Foskett, J. K.; Hallows, K. R. *Am. J. Physiol. Cell Physiol.* **2009**, *296*, C672–C681. (c) Wang, L.; Schultz, P. G. *Angew. Chem., Int. Ed.* **2005**, *44*, 34–66.
- (6) Doherty, M.; Belcher, C.; Regan, M.; Jones, A.; Ledingham, J. *Ann. Rheum. Dis.* **1996**, *55*, 432–436.
- (7) Xu, S.; He, M.; Yu, H.; Cai, X.; Tan, X.; Lu, B.; Shu, B. *Anal. Biochem.* **2001**, *299*, 188–193.
- (8) Ronaghi, M.; Uhlen, M.; Nyrén, P. *Science* **1998**, *281*, 363–365.
- (9) (a) Shao, N.; Wang, H.; Gao, X.; Yang, R.; Chan, W. *Anal. Chem.* **2010**, *82*, 4628–4636. (b) Ojida, A.; Takashima, I.; Kohira, T.; Nonaka, H.; Hamachi, I. *J. Am. Chem. Soc.* **2008**, *130*, 12095–12101. (c) Lee, H. N.; Xu, Z.; Kim, S. K.; Swamy, K. M. K.; Kim, Y.; Kim, S.-J.; Yoon, J. *J. Am. Chem. Soc.* **2007**, *129*, 3828–3829. (d) Nishizawa, S.; Kato, Y.; Teramae, N. *J. Am. Chem. Soc.* **1999**, *121*, 9463–9464.
- (10) (a) Lee, D. H.; Im, J. H.; Son, S. U.; Chung, Y. K.; Hong, J.-I. *J. Am. Chem. Soc.* **2003**, *125*, 7752–7753. (b) Rhee, H.-W.; Choi, S. J.; Yoo, S. H.; Jang, Y. O.; Park, H. H.; Pinto, R. M.; Cameselle, J. C.; Sandoval, F. J.; Roje, S.; Han, K.; Chung, D. S.; Suh, J.; Hong, J.-I. *J. Am. Chem. Soc.* **2009**, *131*, 10107–10112. (c) Kim, S. K.; Lee, D. H.; Hong, J.-I.; Yoon, J. *Acc. Chem. Res.* **2008**, *42*, 23–31.

# **Scheme 1. Proposed Mechanism of the ECL-Based PPI Sensing**



precursors, and subsequently, ECL emission occurs via radiative relaxation.<sup>11</sup> This method is different from the existing optical PPI detection methods because ECL requires no external light source but is initiated and controlled by electrochemical turn-on. Moreover, the electrochemical approach is less expensive than conventional sensing methods and allows for efficient control of the emission time and position of the emission maximum.<sup>12</sup> In addition, ECL devices can be easily miniaturized.

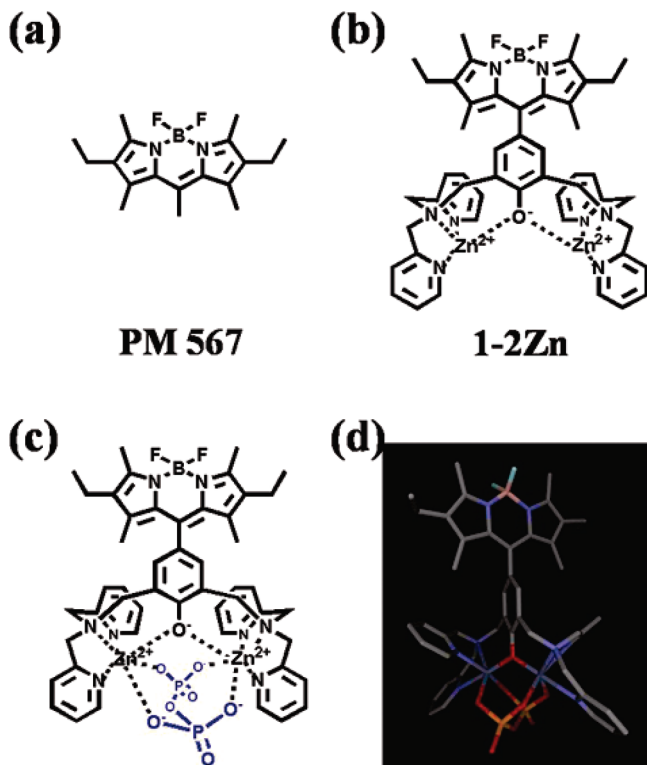
ECL has been widely studied in bioanalysis and DNA determination.<sup>13</sup> Some of them have already been commercialized and used in immunoassays.<sup>14</sup> The most common feature of ECL analysis is the use of tris(2,2'-bipyridine) ruthenium(II) ( $\text{Ru}(\text{bpy})_3^{2+}$ ) or one of its derivatives as the emissive label and tri-*n*-propylamine (TPrA) as the coreactant. In the ECL analysis system, the presence of an analyte is confirmed by attaching a binding element such as an antibody to a  $\text{Ru}(\text{bpy})_3^{2+}$  analogue; this process results in the generation of ECL in a TPrA solution after separation or washing steps.  $\text{Ru}(\text{bpy})_3^{2+}$  is also used as a

direct emissive reporter for various amines.<sup>11b,13a</sup> Recent advances have shown that ECL can be employed in multiplexed immunoassays.<sup>15</sup> Very recently, Deiss et al. demonstrated that an ECL immunoassay in a microarray format can be used for the simultaneous analysis of multiple bioanalytes.<sup>16</sup> Despite the intensive studies performed and the advances made to ECL analysis, two major challenges remain to be overcome: (1) development of ECL dyes other than  $\text{Ru}(\text{bpy})_3^{2+}$  and (2) pioneering new analytical concepts that enable high-throughput bioanalysis.<sup>17</sup> Although various studies have reported the excellent ECL performance of the  $\text{Ru}(\text{bpy})_3^{2+}$  system, most ECL analyses evidently require separation or washing steps before the detection step. In addition, sophisticated instruments are

- (11) (a) Bard, A. J. In *Electrogenerated Chemiluminescence*; Marcel Dekker, Inc.: New York, 2005. (b) Richter, M. M. *Chem. Rev.* **2004**, *104*, 3003–3036.
- (12) (a) Joo, S.; Brown, R. B. *Chem. Rev.* **2008**, *108*, 638–651. (b) Wang, J. *Acc. Chem. Res.* **2002**, *35*, 811–816. (c) Seidel, M.; Niessner, R. *Anal. Bioanal. Chem.* **2008**, *391*, 1521–1544.
- (13) (a) Miao, W. *Chem. Rev.* **2008**, *108*, 2506–2553. (b) Cao, W.; Ferrance, J. P.; Demas, J.; Landers, J. P. *J. Am. Chem. Soc.* **2006**, *128*, 7572–7578. (c) Miao, W.; Bard, A. J. *Anal. Chem.* **2003**, *75*, 5825–5834. (d) Dennany, L.; Forster, R. J.; White, B.; Smyth, M.; Rusling, J. F. *J. Am. Chem. Soc.* **2004**, *126*, 8835–8841.
- (14) (a) Meso Scale Discovery Home Page. <http://www.mesoscale.com>; accessed 01/09/2010. (b) Roche Diagnostics Corporation Home Page. <http://www.roche.com>; accessed 01/09/2010.

- (15) (a) McGrath, M. F.; Bogosian, G.; Fabellar, A. C.; Staub, R. L.; Vicini, J. L.; Widger, L. A. *J. Agric. Food Chem.* **2008**, *56*, 7044–7048. (b) Krishnan, S.; Hvastkovs, E. G.; Bajrami, B.; Choudhary, D.; Schenkman, J. B.; Rusling, J. F. *Anal. Chem.* **2008**, *80*, 5279–5285.
- (16) Deiss, F.; LaFratta, C. N.; Symer, M.; Blicharz, T. M.; Sojic, N.; Walt, D. R. *J. Am. Chem. Soc.* **2009**, *131*, 6088–6089.
- (17) (a) Kim, J. I.; Shin, I.-S.; Kim, H.; Lee, J.-K. *J. Am. Chem. Soc.* **2005**, *127*, 1614–1615. (b) Oh, J.-W.; Lee, Y. O.; Kim, T. H.; Ko, K. C.; Lee, J. Y.; Kim, H.; Kim, J. S. *Angew. Chem., Int. Ed.* **2009**, *48*, 2522–2524. (c) Omer, K. M.; Bard, A. J. *J. Phys. Chem. C* **2009**, *113*, 11575–11578. (d) Yang, H.; Leland, J. K.; Yost, D.; Massey, R. J. *Nat. Biotechnol.* **1994**, *12*, 193–194. (e) Chang, Y.-L.; Palacios, R. E.; Chen, J.-T.; Stevenson, K. J.; Guo, S.; Lackowski, W. M.; Barbara, P. F. *J. Am. Chem. Soc.* **2009**, *131*, 14166–14167. (f) Hvastkovs, E. G.; So, M.; Krishnan, S.; Bajrami, B.; Tarun, M.; Jansson, I.; Schenkman, J. B.; Rusling, J. F. *Anal. Chem.* **2007**, *79*, 1897–1906. (g) Muegge, B. D.; Richter, M. M. *Anal. Chem.* **2002**, *74*, 547–550. (h) Schmitt, M.; Lin, H.-W. *Angew. Chem., Int. Ed.* **2006**, *46*, 893–896. (i) Berni, E.; Gosse, I.; Badocco, D.; Pastore, P.; Sojic, N.; Pinet, S. *Chem.-Eur. J.* **2009**, *15*, 5145–5152.

**Scheme 2. Chemical Structures of (a) PM567 and (b) 1-2Zn; (c) Proposed Binding Mode of 1-2Zn with PPI; (d) Energy-Minimized Structure of the 1-2Zn–PPI Complex by Spartan 2002**



required for multiplexed bioanalysis because the only orange ECL ( $\sim 630$  nm) of  $\text{Ru}(\text{bpy})_3^{2+}$  is mostly available in ECL analysis. In our approach, an ECL reporter selectively recognizes an analyte and reports its existence by the change in the ECL intensity. Therefore, it allows a target-specific ECL analysis without any separation and washing steps. Anion sensing using green ECL would offer an additional advantage to the current ECL analysis.

## RESULTS AND DISCUSSION

We synthesized a PPI sensor (1-2Zn) comprising an emissive ECL reporter unit (boron dipyrromethene (PM567)) and a PPI receptor unit (phenoxo-bridged bis( $\text{Zn}^{2+}$ –dipicolylamine) complex = pbZn–DPCA;  $\text{Zn}_2(2,6\text{-bis}[N,N'\text{-di}(2\text{-pyridylmethyl})\text{aminomethyl}]\text{phenolate})(\mu\text{-hydroxo})$ , dipicolylamine = DPCA), as shown in Scheme 2, parts a and b. The energetic characteristics of PM567 enable the efficient population of the excited states of this moiety in TPrA solution under the applied potential and the subsequent generation of green ECL.<sup>18</sup> The receptor unit, i.e., the pbZn–DPCA moiety, selectively binds to PPI by forming a bridge between two  $\text{Zn}^{2+}$  cations and a PPI anion to afford two hexacoordinated  $\text{Zn}^{2+}$  complexes (Scheme 2c). The electron density on the nitrogen atoms of the two DPCA moieties in pbZn–DPCA increases upon binding with PPI, and this leads to attenuation of the ECL emission from the singlet-excited states of the PM567 moiety. The calculated chemical structure of 1-2Zn clearly reveals that the PM567 and pbZn–DPCA moieties are

orthogonally bonded to each other (Scheme 2d). The electronic states of the aforementioned moieties are isolated, and hence, only intramolecular through-space electron transfer is allowed.<sup>19</sup> Therefore, in the absence of PPI, the electronic states of PM567 are not influenced by the pbZn–DPCA moiety, and thus, intense ECL is produced by PM567. However, when PPI is present in the solution, a pbZn–DPCA–PPI binding complex is formed, and consequently, there is an increase in the electron density on the nitrogen atoms of the two DPCA moieties in pbZn–DPCA. Therefore, complexation between PPI and the pbZn–DPCA moiety of 1-2Zn enables the donation of an electron from the highest-occupied molecular orbital (HOMO) of the complex (1-2Zn and PPI) to the ground state of the excited PM567\* moiety; this subsequently leads to quenching of the ECL emission. Although this process is very similar to photoinduced electron transfer (PET), it is more complicated because the excited states are formed through an electrochemical process between the redox precursors that are also produced via heterogeneous electron transfer from the electrode. In the current system, the pbZn–DPCA–PPI binding complexes not only donate electrons to the excited PM567\* moieties but also decompose partially under the applied potential, and therefore, ECL quenching is achieved both via energetic and electrochemical pathways.

Figure 1a shows the fluorescence spectra of 1-2Zn in aqueous solution (10 mM HEPES buffer, pH 7.4; HEPES = 4-(2-hydroxyethyl)-1-piperazineethanesulfonic acid) and their changes upon the addition of PPI. The fluorescence peak appearing at 536 nm upon the excitation of the PM567 moiety of 1-2Zn is identical to that appearing upon the excitation of PM567; this indicates that the electronic states of PM567 remain unchanged even after the conjugation of this moiety with pbZn–DPCA. The light emission from 1-2Zn decreases upon the addition of PPI. In the absence of PPI, the fluorescence emission from 1-2Zn reaches a maximum at 536 nm and gradually decreases with an increase in the concentration of PPI added. This linear decrease in the fluorescence intensity continues until the PPI concentration is 1 equiv, and then, the fluorescence intensity reaches a plateau (Figure 1b).

Figure 2a shows the ECL spectrum of 1-2Zn in a MeCN solution. The ECL spectrum is recorded by a  $\text{N}_2$ -cooled CCD camera while the potential is swept at a Pt disk electrode (diameter, 2 mm) in the range of 0.3–1.3 V (scan rate, 0.1 V/s). For the ECL experiments, a MeCN solution of 10  $\mu\text{M}$  1-2Zn and 10 mM TPrA (0.1 M TBAPF<sub>6</sub> as a supporting electrolyte) is used. Figure 2b is the cyclic voltammogram of the MeCN solution. As shown in Figure 2a, the ECL spectrum peaks at 545 nm in the green region, and the shape of the spectrum is identical to that of the fluorescence spectrum. The ECL peak is slightly broader and red-shifted compared to the fluorescence peak, mainly because of the differences in the solution conditions and the spectral measurements. 1-2Zn only shows 3.9–4.1% of the ECL intensity of PM567 (vide infra).

A similar tendency to the fluorescence upon the addition of PPI is observed in ECL. The ECL intensity profile is obtained using a low-voltage photomultiplier tube module (operating at 1.0 V)

(18) (a) Sartin, M. M.; Camerel, F.; Ziessel, R.; Bard, A. J. *J. Phys. Chem. C* **2008**, *112*, 10833–10841. (b) Trieflinger, C.; Röhr, H.; Rurack, K.; Daub, J. *Angew. Chem., Int. Ed.* **2005**, *44*, 6943–6947.

(19) (a) Kuimova, M. K.; Yahioglu, G.; Levitt, J. A.; Suhling, K. J. *Am. Chem. Soc.* **2008**, *130*, 6672–6673. (b) D'Souza, F.; Smith, P. M.; Zandler, M. E.; McCarty, A. L.; Ito, M.; Araki, Y.; Ito, O. *J. Am. Chem. Soc.* **2004**, *126*, 7898–7907.



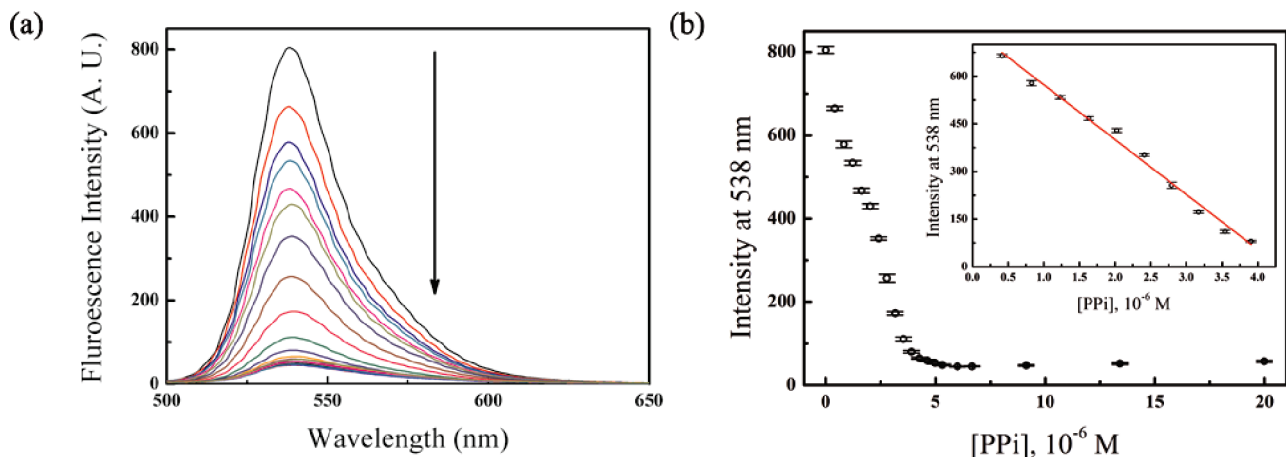


**Figure 1.** (a) Changes in fluorescence spectra obtained for a solution of **1-2Zn** ( $5 \mu\text{M}$ ) in 10 mM HEPES (pH 7.4) at  $25^\circ\text{C}$  upon the addition of increasing amounts of PPI (sodium salt). Excitation wavelength was set at 490 nm. The dashed arrow indicates the increase in PPI concentration.  $[\text{PPI}] = 0, 0.4, 0.8, 1.2, 1.6, 2.0, 2.4, 2.8, 3.2, 3.5, 4.3, 4.6, 5.0, 5.3, 6.0, 6.7, 9.1, 13.4$ , and  $20 \mu\text{M}$ . (b) Changes in fluorescence intensity of **1-2Zn** at 540 nm upon the addition of PPI. Inset: linear relationship between fluorescence intensity and PPI concentration ( $R^2 = 0.99$ ).

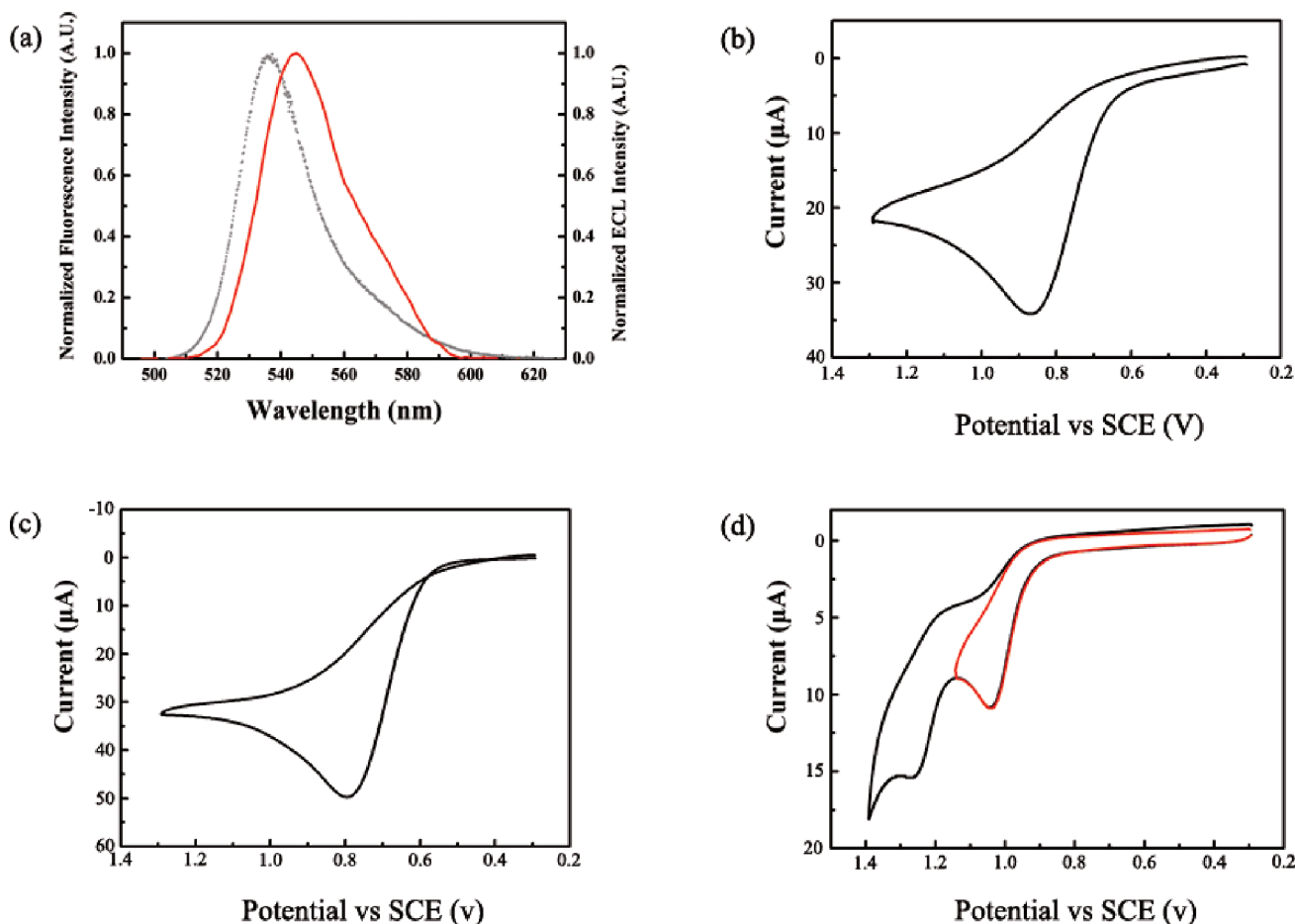


**Figure 2.** (a) ECL spectrum of a solution of  $10 \mu\text{M}$  **1-2Zn** in MeCN (10 mM TPrA and 0.1 M  $\text{TBAPF}_6$  as supporting electrolyte) while the potential is repeatedly swept at a Pt disk electrode (diameter, 2 mm) in the range of 0.3–1.3 V (scan rate, 0.1 V/s) (red line) and fluorescence spectrum of a solution of  $5 \mu\text{M}$  **1-2Zn** in 10 mM HEPES buffer (pH 7.4) (gray dotted line). (b) Cyclic voltammogram of a solution of  $10 \mu\text{M}$  **1-2Zn** in the presence of 10 mM TPrA (0.1 M  $\text{TBAPF}_6$  as supporting electrolyte; scan rate, 0.1 V/s). (c) Cyclic voltammogram of a solution of 10 mM TPrA in MeCN. (d) Cyclic voltammogram of a solution of 2 mM **1-2Zn** (red line, scan from 0.3 to 1.15 V; black line, scan from 0.3 to 1.4 V).

during the potential sweep. Upon increasing the PPI concentration, the ECL intensity gradually decreases and is almost quenched when the concentration reaches 2 equiv (Figure 3a). The binding between pbZn–DPCA and PPI is assumed to influence the excited PM567\* moiety, as in the case of fluorescence, and facilitates ECL

quenching via a nonradiative pathway. Figure 3b shows the isothermal binding curve plotted using the data collected during the ECL titration of **1-2Zn** at various PPI concentrations. The binding curve indicates that the ECL intensity shows a linear correlation with the PPI concentration in the range of 6.6–13.3

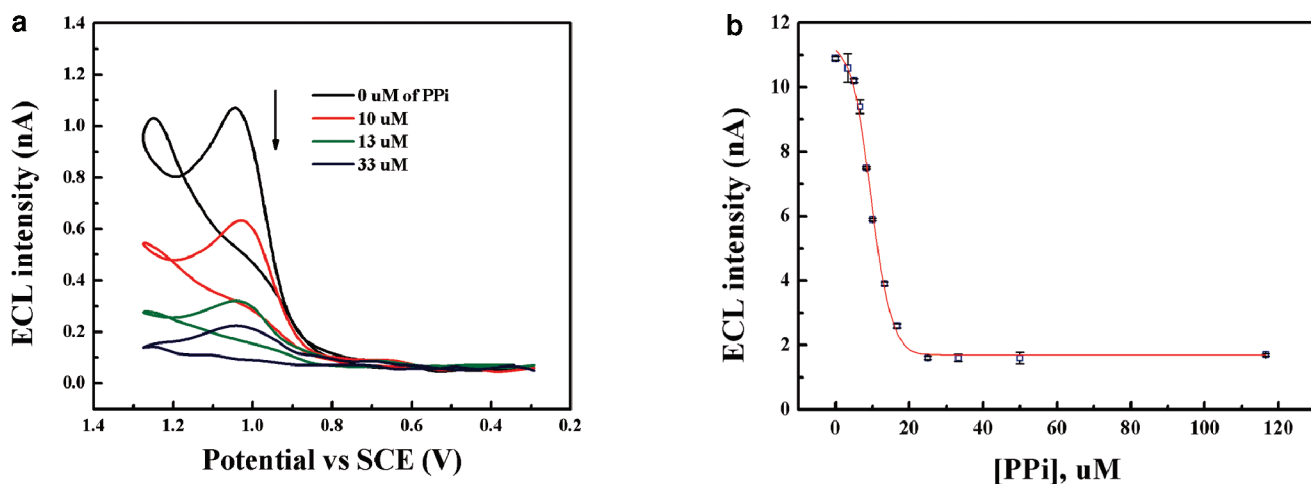


**Figure 3.** (a) ECL intensity of 10  $\mu\text{M}$  **1-2Zn** upon the addition of PPI in MeCN (10 mM TPrA and 0.1 M TBAPF<sub>6</sub> as supporting electrolyte) while the potential is swept at a Pt disk electrode (diameter, 2 mm) in the range of 0.3–1.3 V (scan rate, 0.1 V/s). (b) Isothermal binding curve obtained for ECL titration upon the addition of PPI (10  $\mu\text{M}$  **1-2Zn**, 10 mM TPrA, and 0.1 M TBAPF<sub>6</sub> in MeCN).

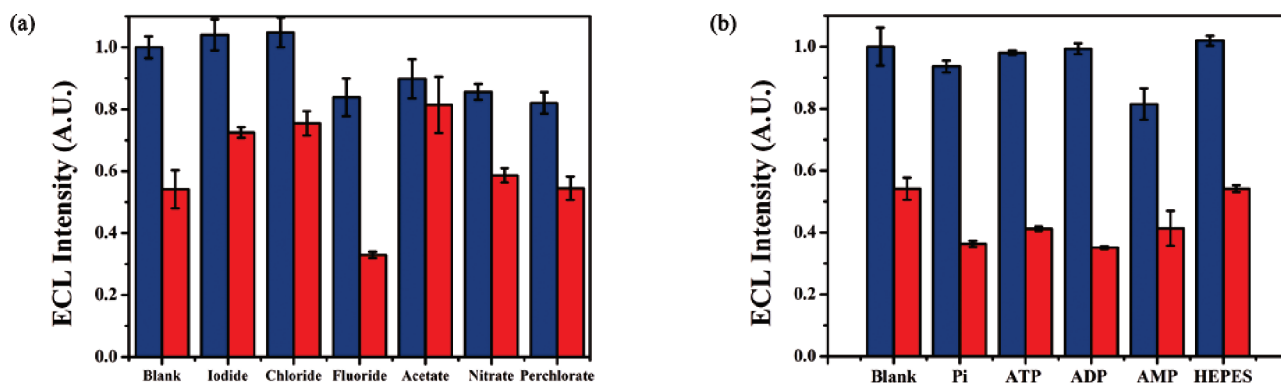


**Figure 4.** Competitive binding assays performed by the addition of 10  $\mu\text{M}$  PPI to 10  $\mu\text{M}$  **1-2Zn** in the presence of (a) 100  $\mu\text{M}$  anions and (b) 10  $\mu\text{M}$  Pi-containing anions (10  $\mu\text{M}$  **1-2Zn**, 10 mM TPrA, and 0.1 M TBAPF<sub>6</sub> in MeCN). No significant change is observed in the ECL intensity (blue bars), whereas the addition of PPI causes a notable decrease in the ECL intensity (red bars).

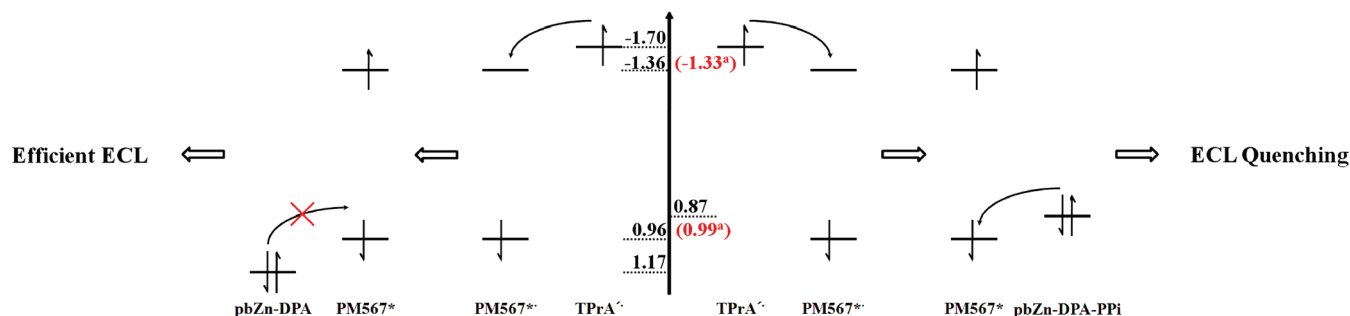
$\mu\text{M}$  when the **1-2Zn** concentration is constant at 10  $\mu\text{M}$  ( $R^2 = 0.99$ ,  $y = (8.2 \times 10^{-5})x - 3.5 \times 10^{-10}$ ). The estimated limit of detection is 4.0  $\mu\text{M}$  (signal/noise ratio = 3,  $n = 5$ ). The binding curve is slightly different from that obtained during the fluorescence titration in that it has a sigmoidal shape and is linear for a little narrow range of PPI concentration. There are several possible reasons for this difference. First, at high concentrations, TPrA can compete with PPI and form a weak bond with pbZn–DPCA, thus interfering with the effective binding of pbZn–DPCA with PPI. Second, all the molecules in solution are consistently under the influence of the applied potential, and hence, the PPI binding in this case cannot be the same as that under fluorescence conditions. In addition, upon binding with PPI, pbZn–DPCA undergoes the irreversible electrochemical oxidation before the oxidation of the PM567 moiety, which indicates **1-2Zn** may be partially decomposed under the applied potential. Therefore, the ECL intensity varies slightly with an increase in the PPI concentration, yielding a nonlinear quenching curve; at low PPI concentrations, the ECL intensity slowly decreases and is almost saturated when the concentration becomes 2 equiv.

The selectivity of **1-2Zn** to PPI in the presence of other anions is evaluated by a competitive binding assay, which is performed by adding 10  $\mu\text{M}$  PPI to 10  $\mu\text{M}$  **1-2Zn** in the presence of 100  $\mu\text{M}$

of other anions. The experimental results show that the ECL intensity of **1-2Zn** slightly changes upon the addition of 10-fold excess of other anions but significantly decreases when only 1 equiv of PPI was added to the solution (Figure 4a). As anions form weak complexes with pbZn–DPCA, ECL intensity of **1-2Zn** decreases upon their excessive presence in the solution. The slight increase in ECL intensity upon excessive addition of I<sup>−</sup> or Cl<sup>−</sup> is hardly explainable because there is no reported result related to it. As shown in Figure 4b, no notable change is observed in the ECL intensity in the presence of phosphate (Pi) anions and Pi-containing anions such as adenosine-5'-triphosphate (ATP), adenosine diphosphate (ADP), and adenosine monophosphate (AMP), whereas the ECL intensity decreases considerably upon the addition of PPI. The higher selectivity for PPI can be explained on the basis of the structure of pbZn–DPCA and the charge density on the oxygen atoms bonded to phosphorus of the guest anions involved in complexation. For example, the total anionic charge density on the four O–P oxygen atoms involved in the complexation of the Pi-containing anions with **1-2Zn** is lower than that on the four O–P oxygen atoms of PPI.<sup>20</sup> Therefore, the binding affinity of Pi is drastically reduced, and the change in the

(20) Lee, D.-H.; Kim, S. Y.; Hong, J.-I. *Angew. Chem., Int. Ed.* **2004**, *43*, 4777–4780.

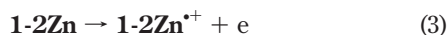
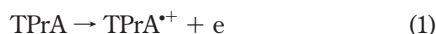
### Scheme 3. Thermodynamic Explanation for ECL PPI Sensing by **1-2Zn**<sup>a</sup>



<sup>a</sup> Energetic values of PM567 show a slight shift when this moiety is incorporated into **1-2Zn**. The reduction potentials of PM567 moiety (−1.36 and −1.33 V) were calculated by considering the emission maximum of **1-2Zn** in the fluorescence spectrum.

ECL intensity becomes less significant when the Pi-containing anions bind to **1-2Zn**.

In order to investigate the ECL mechanism, we performed an electrochemical study. Figure 2, parts c and d, and Supporting Information Figure S1, parts a and b, show the cyclic voltammograms of TPrA, **1-2Zn**, PM567, and pbZn–DPCA, respectively. As shown in Figure 2d, **1-2Zn** undergoes two irreversible oxidations at  $E_{\text{ox},1/2} = 0.99$  and 1.22 V. On the basis of the oxidation behaviors of PM567 and pbZn–DPCA (in Supporting Information Figure S1), the first oxidation wave observed for **1-2Zn** is attributed to the oxidation of the PM567 moiety. PM567 undergoes near-Nernstian oxidation at  $E_{\text{ox},1/2} = 0.96$  V ( $i_{\text{pc}}/i_{\text{pa}} = 1.00$ ,  $\Delta E_{\text{pp}} = 81$  mV at the scan rate of 0.1 V/s), but covalent conjugation of this moiety to the pbZn–DPCA moiety in **1-2Zn** leads to partial loss of the reversibility of the oxidation reaction at  $E_{\text{ox},1/2} = 0.99$  V ( $i_{\text{pc}}/i_{\text{pa}} = 0.18$ ,  $\Delta E_{\text{pp}} = 84$  mV). The electron-deficient pbZn–DPCA probably stabilizes the HOMO of the PM567 moiety in **1-2Zn**, and consequently, the oxidation potential becomes slightly more positive.<sup>21</sup> As TPrA is directly oxidized at around ~0.8 V (Figure 2c), the oxidation of TPrA is expected to precede the oxidation of **1-2Zn** to its cationic form in solution. The ECL intensity reaches a maximum at 1.05 V (Figure 3a), where the peak current of the anodic wave of **1-2Zn** is observed (Figure 2d). This supports the assumption that ECL emission mainly depends on the direct oxidation of PM567 in **1-2Zn**. Thus, our system is considered that the ECL intensity normally depends on the direct oxidation of ECL dyes.<sup>22</sup> The ECL mechanism is proposed as follows.



Thermodynamic considerations confirm the efficient formation of excited singlet states in **1-2Zn** via the ECL process. The total free energy for the electron transfer is calculated in terms of the

half-wave potentials of **1-2Zn** and the TPrA<sup>•</sup> radical after correction for entropy effects (0.1 eV):  $\Delta G^0 = \Delta H^0 - T\Delta S^0 = E_{1/2}(\text{TPrA}^{\bullet} \text{ radical}) - E_{\text{ox},1/2}(\mathbf{1-2Zn})$ . From the recently estimated reducing power of the TPrA radical ( $E_{1/2}(\text{TPrA}^{\bullet} \text{ radical}) = -1.7$  V against SCE),<sup>23</sup> the enthalpy change ( $\Delta H^0$ ) is calculated to be −2.6 eV ( $= (-1.7) - 0.99 + 0.1$ ), which is sufficient to cause singlet excitation ( $E_s = 2.3$  eV) in PM567, as determined from the fluorescence spectral measurements. Thus, it is concluded that, in the presence of TPrA, the excited states in **1-2Zn** are efficiently populated via electrochemical oxidation.

The obtained electrochemical data also provide information on changes in the ECL intensity. When PPI binds to pbZn–DPCA, there is an increase in the electron density on the two nitrogen atoms of the amine moiety in the latter. This leads to destabilization of the HOMO of pbZn–DPCA. In order to investigate the variations in the pbZn–DPCA HOMO energy, we studied the oxidation behavior of the DPCA molecule upon successive addition of Zn<sup>2+</sup> and PPI. As shown in Supporting Information Figure S2, the first oxidation potential of DPCA ( $E_{\text{ox},1/2} = 0.83$  V) corresponds to the HOMO level of the amine moiety in DPCA, and this potential becomes more positive ( $E_{\text{ox},1/2} = 1.17$  V) upon the addition of Zn<sup>2+</sup>. After the addition of PPI,  $E_{\text{ox},1/2}$  decreases to 0.87 V, which is almost equal to the original value (0.83 V). The incorporation of Zn<sup>2+</sup> into the DPCA moiety leads to stabilization of the HOMO of DPCA via a decrease in the electron density on the nitrogen atoms of DPCA, and hence, the oxidation potential becomes more positive (Supporting Information Figure S2b). However, when PPI is added to the solution, it donates electrons to the Zn<sup>2+</sup> cations by forming a bridge with Zn<sup>2+</sup>; as a result, the HOMO of DPCA is destabilized, and the electron density on the amine moieties of DPCA increases. Therefore, the DPCA oxidation peak at  $E_{\text{ox},1/2} = 0.83$  disappears when DPCA binds to the incorporated Zn<sup>2+</sup> cation and reappears when PPI is added. On the basis of the obtained electrochemical data, the generation and quenching of ECL can be explained from the viewpoint of thermodynamics (Scheme 3). The electronic states of **1-2Zn** correspond to those of PM567 and pbZn–DPCA. Since these two moieties are bonded in an orthogonal fashion, their electronic states are independent of each other, and thus, only electron-transfer reactions are allowed. Therefore, in the absence of PPI, **1-2Zn** efficiently generates ECL in TPrA solution. In the presence of PPI, however, the HOMO of the pbZn–DPCA moiety is elevated to a higher

(21) Lai, R. Y.; Bard, A. J. *J. Phys. Chem. B* **2003**, *107*, 5036–5042.

(22) Miao, W.; Choi, J.-P.; Bard, A. J. *J. Am. Chem. Soc.* **2002**, *124*, 14478–14485.

(23) Lai, R. Y.; Bard, A. J. *J. Phys. Chem. A* **2003**, *107*, 3335–3340.

energy level because of PPI binding. This enables electron donation from pbZn–DPCA to the half-filled ground state of the excited PM567\* moiety. Hence, upon the addition of PPI, ECL quenching occurs via through-space electron transfer from pbZn–DPCA to PM567\*. In addition, the irreversible oxidation of the pbZn–DPCA–PPI complex at 0.87 V indicates that **1-2Zn** may be partially decomposed before the oxidation of the PM567 moiety. Thus, we conclude that the electrochemical decomposition of the pbZn–DPCA–PPI binding complex also contributes to the decrease in the intensity of ECL emission from **1-2Zn**.

## CONCLUSION

In conclusion, the ECL sensor (**1-2Zn**) comprising PM567 (ECL reporter) and pbZn–DPCA (receptor unit) selectively recognizes and detects PPI on the basis of variations in the light emission by electrochemical turn-on. **1-2Zn** generates green ECL via an electrochemical process because of the energetic and electrochemical characteristics of PM567 in TPrA solution. Upon the presence of PPI, the complexation between PPI and the pbZn–DPCA moiety of **1-2Zn** enables the donation of an electron from the HOMO of the complex (**1-2Zn** and PPI) to the ground state of the excited PM567\* moiety; this subsequently leads to quenching of the ECL emission. The electrochemical irreversibility of pbZn–DPCA–PPI binding complex also contributes to ECL quenching. ECL experiments presented here are performed in MeCN because ECL generation is not observed in 100% aqueous solutions. However, the similar result is also observed in the mixed

solutions of MeCN and water, which is not shown here. Apparently, the development of water-stable ECL sensors should enable ECL sensing of PPI in aqueous solutions. In the present study, we demonstrate electrochemically controllable anion sensing, which is a combination of spectroscopic and electrochemical methods. Because of its unique characteristics and potential applications in specific molecular sensing, we expect our ECL sensing approach to emerge as a useful strategy for molecular sensing and ECL analysis.

## ACKNOWLEDGMENT

This study was supported by the NRF Grant funded from the MEST (Grant No. 2009-0080734) and Seoul R&BD (10543). A partial support was provided by the Basic Science Research Program through the NRF Grant funded from the MEST for the Center for Next-Generation Dye-Sensitized Solar Cells (No. 2010-0001842). The first two authors contributed equally to this work.

## SUPPORTING INFORMATION AVAILABLE

Synthesis, characterization, electrochemical measurement, and electrochemical data (Figures S1, S2, and Table S1). This material is available free of charge via the Internet at <http://pubs.acs.org>.

Received for review June 30, 2010. Accepted August 28, 2010.

AC1017293